EARTHQUAKE ENGINEERING AND STRUCTURAL DYNAMICS, VOL. 26, 1209–1229 (1997)

STABILITY OF ELEVATED LIQUID-FILLED CONICAL TANKS UNDER SEISMIC LOADING, PART II—APPLICATIONS

A. A. EL DAMATTY,[1]* R. M. KOROL[2] AND F. A. MIRZA[2]

[1]*Department of Civil Engineering, The University of Western Ontario, London, Ontario, Canada N6A 5B9*
[2]*Department of Civil Engineering, McMaster University, Hamilton, Ont., Canada*

SUMMARY

In this paper, the numerical model developed in the previous paper is used to study the seismic performance of elevated liquid-filled steel conical tanks. A number of conical tanks which are classified as tall or broad tanks according to the ratio of the tank radius to its height are considered. The consistent shell element is used to model the tank surfaces, while the coupled boundary-shell element formulation is employed to obtain the fluid added-mass which simulates the dynamic pressure resulting from a seismic motion. Linear springs are used to model the supporting towers. The natural frequencies of the liquid-filled tanks due to both horizontal and vertical excitations are evaluated. This is followed by a non-linear dynamic analysis, using an appropriately scaled real input ground motion, and which includes the effect of both geometric and material non-linearities. Thin-walled structures of this kind may exhibit inelastic behaviour and a tendency to develop localized buckles, thus diminishing stiffness. The consequence could lead to overall instability of the structure. In general, time-history analyses indicate that liquid-filled conical tanks, often possessing apparently adequate safety factors under hydrostatic loading, are shown to be very sensitive to seismic loading when ground motion frequencies contain those of the fundamental frequencies of the vessels themselves.

Earthquake Engng. Struct. Dyn., **26**, 1209–1229 (1997)

No. of Figures: 14. No. of Tables: 2. No. of References: 15.

KEY WORDS: tanks; vessels; conical; seismic; earthquake; stability; shells; finite element; boundary element

1. INTRODUCTION

The truncated cone with cylinder superimposed on top is commonly used as the shape of elevated water tanks in North America and Europe. As previously described in the companion paper,[1] this type of structure is usually a steel thin-walled vessel supported by a circular steel plate resting on a heavily reinforced concrete slab. To obtain the needed height for achieving the supply of water by gravity, such a structure is normally supported by a reinforced concrete tower.

In December 1990, a liquid-filled conical tank located at Fredericton, Canada, failed dramatically when it was being filled with water for the first time. Figure 1 shows a photograph of the partially painted superstructure before filling took place, while a sense of the explosive nature of collapse is evident from Figure 2.

Although, the failure was under static conditions, it drew the authors' attention to the applicable design code for seismic loading, which in this case was based on the American Water Works Association Specification AWWA-D100.[2] It became evident that this standard did not include any guidance for undertaking a meaningful seismic analysis and associated design of this type of containment vessel. Indeed, no provisions for seismic design of these water structures are available in the current draft of the 1996 AWWA specifications. Moreover, it was discovered that no previous analytical or experimental studies had been attempted to investigate the seismic performance of conical tanks. However, several studies dealing with

* Correspondence to: A. A. El Damatty, Department of Civil Engineering, The University of Western Ontario, London, Ontario, Canada N6A 5B9

CCC 0098–8847/97/121209–21$17·50

Received 23 April 1996
Revised 5 June 1997

Figure 1. Completed Fredericton tank prior to filling

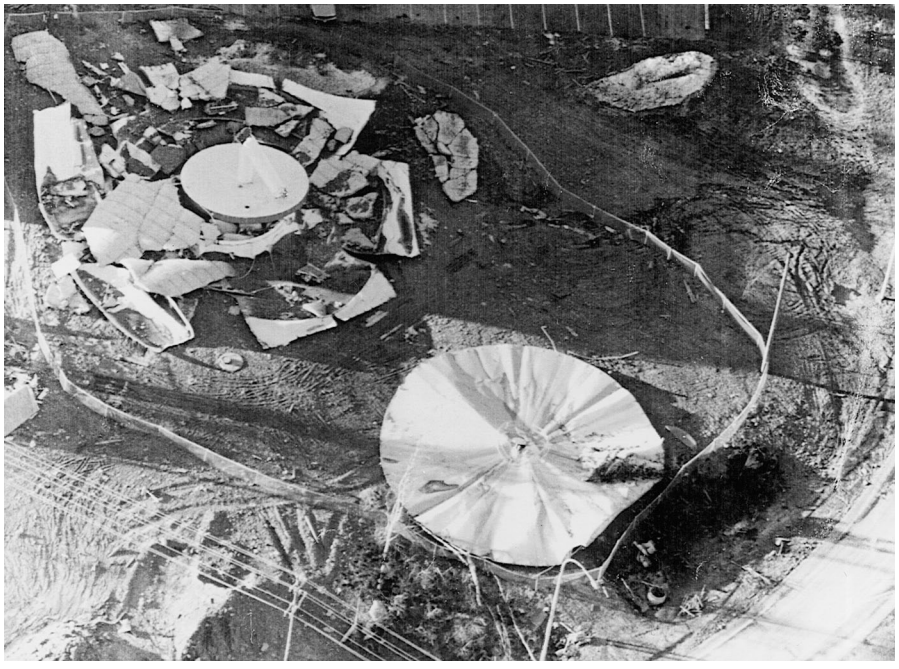

Figure 2. Aerial view of Fredericton tower collapse

the seismic behaviour of cylindrical tanks served as a guide to evaluating the performance of conical tanks. Full details of this history and the demise of the structure can be found in Reference 3.

In the case of fluid-filled cylindrical tanks, a number of analytical studies have been carried out on fluid-filled cylindrical tanks to determine the hydrodynamic pressures resulting from earthquake excitation. In these investigations, linear analyses were used to evaluate the displacements, the base shear and the overturning moment induced by the horizontal component of ground motion. These studies focused mainly on ground tanks, however one study was presented by Haroun and Ellaithy[4] in which the linear elastic response of an elevated cylindrical tank was studied. Indeed, two examples were considered in their study: a small capacity tank resting on a cross braced frame and a larger tank supported by a pedestal tower. Both the response spectra and time-history analyses show that the flexibility of a tank is important for large capacity cylindrical vessels. These analyses also indicated that the rocking motion exhibited by pedestal-type supported tanks has an important effect on the behaviour.

Concerning the effect of vertical acceleration on cylindrical tanks, very few studies can be found in the literature. In this regard, Haroun and Tayel[5] concluded from their analytical study on ground-based cylindrical tanks that the axial stresses induced by the vertical acceleration component can be neglected compared to those resulting from the horizontal component. However, they also mentioned that the increase of hoop stresses due to the vertical acceleration would be important when accounting for material non-linearity.

The performance of cylindrical tanks during actual earthquakes has been recorded in a number of investigations, e.g. References 6–8. One of the common forms of damage found to occur was buckling of the vessel walls near their bases resting on the ground. Such localized instability is mainly due to the overturning moment which is exerted by the hydrodynamic pressure caused by the horizontal component of the earthquake motion.

Returning to conical shell containment vessels, it is expected that the horizontal ground accelerations would also cause significant overturning moment at the base of the cone. This overturning moment will have an amplifying effect on their tendency to instability due to the small radius at the bottom. Also, due to the inclination of the walls of the cone, vertical accelerations are expected to induce both axial and hoop stresses in the shell. As such, the vertical component of the ground acceleration may be expected to have an important effect on such a tank's stability, and hence needs to be considered in any seismic analysis.

It should be noted that previous studies have shown that the stresses at the base of cylindrical tanks resulting from seismic motion are usually less than the yield stress of the steel. As such, it seems reasonable to consider only the linear response of such structures in seismic analysis. However, for the case of liquid-filled conical steel tanks, the meridional stresses due to hydrostatic pressure, when added to those resulting from seismic excitation, may indeed lead to yielding. This plastification, together with localized large deformations near the base, may cause premature local buckling near the bottom of the tank, followed by overall instability of the structure. It seems prudent, therefore, to include geometric and material non-linearities when performing seismic analysis on liquid-filled conical tanks.

In this paper, the numerical model developed in the companion paper (El Damatty *et al.*[1]) is used to study the seismic performance of a number of liquid-filled elevated steel conical tanks. The vessels considered are classified as 'broad' or 'tall' according to the superstructure dimensions. A free vibration analysis was first conducted to predict the natural frequencies of the liquid-filled tanks due to both horizontal and vertical excitations. Using the horizontal and vertical components of an appropriately scaled real input ground motion, the finite-boundary element model developed in the companion paper is used to study the dynamic stability of the liquid-filled tanks through a non-linear time-history analysis.

2. STATIC ANALYSIS

As a response to an earlier collapse of a conical tank in Belgium during the 1970s, an extensive experimental investigation for the stability of conical tanks under hydrostatic loading was developed by Vandepitte *et al.*[9]

Later, a comprehensive numerical study of the same problem was carried out by El Damatty *et al.*[10] In the seismic analysis presented in this study, a static load factor p_{cr} which was used by both Vandepitte *et al.* and El Damatty *et al.* in their static analyses will serve as a baseline to judge the sensitivity of a given structure to seismic loading. The static load factor for a given shell geometry is defined as that hydrostatic pressure associated with a fluid depth h, to cause the vessel to be on the verge of failure. As such, it is important before conducting a dynamic analysis to discuss how the hydrostatic pressure might lead to instability of conical tanks and then to describe how the static load factor can be quantified.

2.1. *Instability of conical tanks under static conditions*

To understand the cause of failure of conical tanks subjected to hydrostatic loading, consider the liquid-filled elevated conical tank shown in Figure 3(a). Note that upper cylindrical segment typical for elevated water towers (Figure 1) has been omitted for reasons of simplification. Assume the existence of an imaginary vertical cylinder inside the tank of radius equal to the bottom radius of the conical tank and extending the whole height of the tank. Consider the volume of the liquid bounded by the surface of this imaginary cylinder and the surface of the conical tank (shown hatched). The weight of the liquid in this volume of revolution is equilibrated by high compressive meridional stresses σ, in the bottom part of the shell (Figure 3(b)) which could lead to buckling despite a stabilizing effect brought about by tensile hoop stresses in that region. Geometric imperfections, always present in real shell structures, will tend to exacerbate the situation, and may be precipate instability earlier than would be the case of a perfect tank.

2.2. *Method of static analysis and determination of* P_{CR}

An in-depth study of the stability of liquid-filled conical tanks under hydrostatic loading has recently been reported.[10] In this investigation, a consistent shell element formulated by Koziey and Mirza[11] and extended to include non-linear analysis by El Damatty,[12] was used for the modelling of conical tanks. The finite element model, having both geometric and material non-linearities included, allows non-linear stability analysis of liquid-filled conical tanks in both the elastic and the inelastic ranges to be performed. This is achieved by gradually increasing the load acting on the tank wall. The stiffness of the tank will correspondingly decrease with an increase in load until the limit load is reached, i.e. the stiffness vanishes. In the analysis, the structure is assumed to be filled with water. To start the numerical analysis, the hydrostatic pressure is multiplied by a load factor p which is increased until the structure reaches its limit load p_{cr}, the critical load factor. Now $p_{cr} = 1$ corresponds to the real situation of a tank filled with water and on the verge of failure.

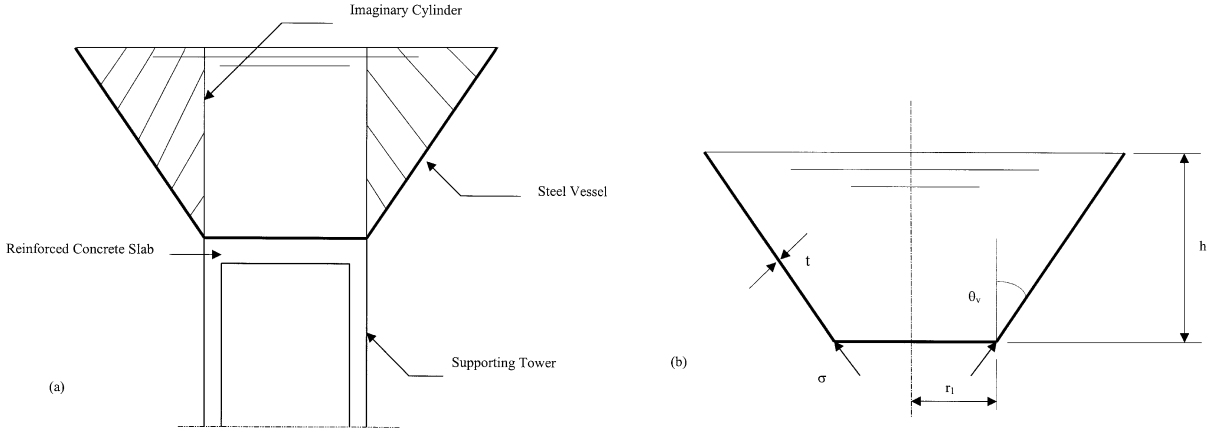

Figure 3. (a) Cross-sectional elevation of an idealized conical tank; (b) meridional stresses due to hydrostatic loading

If p_{cr} is less than unity, then the structure cannot sustain the hydrostatic load, while a value larger than unity signifies that such a loading can be sustained. Indeed, p_{cr} becomes the partial safety factor for the tank when it is filled with water.

2.3. Geometric imperfections

Geometric imperfections play an important role in determining the limit load capacity of real shells. In the study done by El Damatty *et al.*,[10] the effect of both axisymmetric and non-axisymmetric imperfections on the stability of conical tanks subjected to hydrostatic loading was investigated. Analyses have shown that axisymmetric imperfections leads to the lowest limit loads of a tank. An axisymmetric imperfection wave having a unit thickness amplitude and a wavelength equal to the wavelength of the buckling mode of the structure leads to about a 40 per cent reduction of a tank's limit load.

In the following dynamic analysis, the geometric imperfections due to fabrication were assumed to be axisymmetric and to be mathematically described by the following equation:

$$w^* = w_0 \sin\left(\frac{2\pi S}{l_r}\right) \tag{1}$$

where w^* is the imperfection perpendicular to the tank surface; w_0 is the amplitude of the imperfection wave; S is the distance measured along a generator of the tank; and l_r is the wavelength of the imperfection and assumed to be equal to the wavelength of the first buckling mode of the perfect tank. These imperfections are introduced into the finite element model as initial strains existing in the structure before applying the load.

3. EFFECT OF HORIZONTAL EXCITATION ON CONICAL TANKS

As mentioned in Section 4.1 of the companion paper (El Damatty *et al.*[1]), a horizontal excitation results in a $\cos\theta$-type variation of the hydrodynamic pressure in the circumferential direction. This dynamic pressure distribution is symmetric about the x-axis (Figure 4(a)). Its variation about the y-axis leads to two resultant forces, P, normal to the surface of the tank. The first resultant acts downward at a certain location on the generator defined by $\theta = 0$ and the second resultant acts upward at a similar location on the generator defined by $\theta = 180$. These two forces exert a base shear and an overturning moment at the base of the conical tank which could lead to plastification or to dynamic instability of the tank.

4. EFFECT OF VERTICAL EXCITATIONS ON CONICAL TANKS

A vertical acceleration acting on a liquid-filled conical tank is expected to lead to an axisymmetric dynamic pressure distribution as shown in Figure 4(b). Due to this dynamic pressure, upward and downward vertical accelerations will exert added compressive and reduced compressive meridional forces on the tank, respectively. Thus, unlike the case of liquid-filled cylindrical tanks, the vertical acceleration is expected to have an important contribution on the dynamic stability of a liquid-filled conical tank and, therefore, it is important to consider the vertical component of an earthquake when performing seismic analysis of liquid-filled conical tanks.

5. LAYOUT OF CONICAL TANKS USED IN THE DYNAMIC ANALYSIS

The seismic behaviour of liquid-filled conical shaped tanks will be investigated using the numerical model developed in the companion paper (El Damatty *et al.*[1]). Seven different superstructure geometries are considered in the dynamic analysis. All seven tanks are assumed to be full cones. The tanks are classified as broad or tall according to the ratio of their height to their bottom radius. The first tank (B1) is classified as broad while the other six are classified as tall. The dimensions of the tanks are given in Table I with symbols

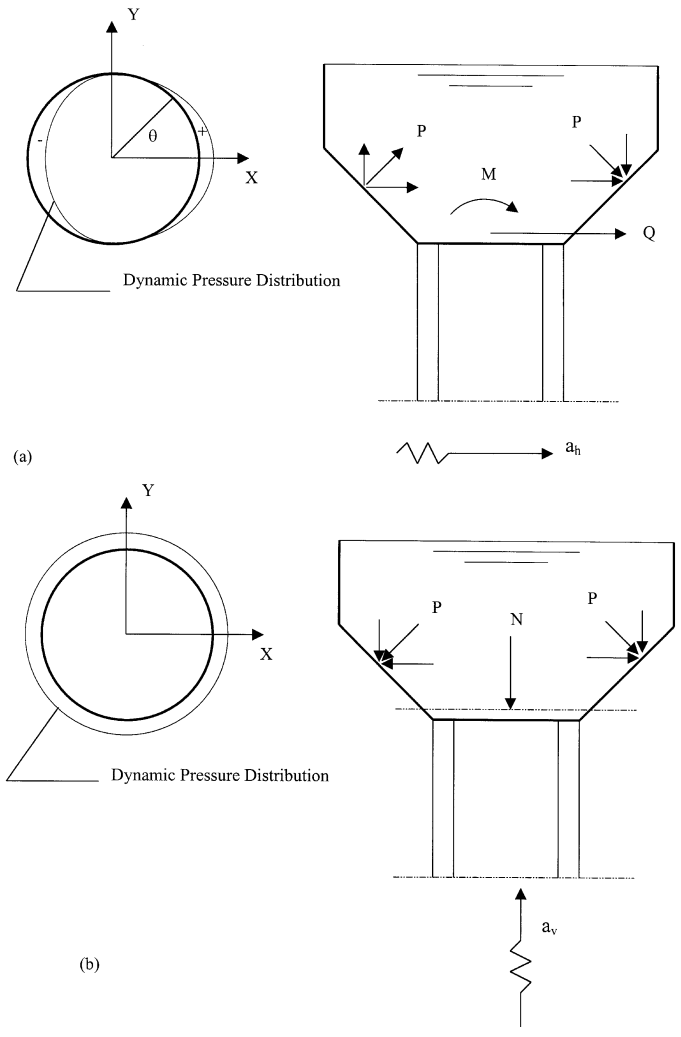

Figure 4. (a) Effect of horizontal acceleration on conical tanks; (b) effect of vertical acceleration on conical tanks

defined in Figure 3(a). As will be noted, tanks T1–T6 are essentially the same except for the thickness of the wall which varies from 12 to 16 mm. In the same table, the magnitudes w_0 of the axisymmetric imperfection waves assumed for the tanks are also given. The material properties for all containment vessels were taken as follows: modulus of elasticity $E = 2 \times 10^5$ MPa, tangent modulus $E_T = 6 \times 10^3$ MPa, yield stress $\sigma_y = 300$ MPa, and Poisson's ratio $v = 0{\cdot}3$.

6. MODELLING OF TANKS FOR DYNAMIC ANALYSIS

As previously mentioned, elevated conical tanks usually consist of a steel vessel which is supported by a circular steel plate resting on a heavily reinforced concrete slab supported in turn by a reinforced concrete structure. As such, the base of the vessel can be assumed infinitely rigid and hence can only tilt as a rigid body rotation due to differential axial deformation between the extremities of the concrete tower presumed for this study to consist of rigid frames (see Figure 5(a)). The tilting of the base of the vessel can be neglected due to

Table I. Results of the time history analyses for the conical tanks

Tank	r_1 (m)	h (m)	θ_v	t (mm)	Imperf. (mm)	p_{cr}	Results description
B1	3·0	4·5	60	9·6	9·6	1·5	Safe (plastic)
T1	3·0	9·0	45	12·0	12·0	1·4	Failed (plastic)
T2	3·0	9·0	45	12·0	3·0	2·1	Failed (plastic)
T3	3·0	9·0	45	12·0	0·0	2·25	Failed (plastic)
T4	3·0	9·0	45	13·5	0·0	2·65	Safe (plastic)
T5	3·0	9·0	45	14·0	0·0	2·8	Safe (elastic)
T6	3·0	9·0	45	16·0	7·0	2·8	Safe (elastic)

*Please refer to Figure 3(b) for the notations description

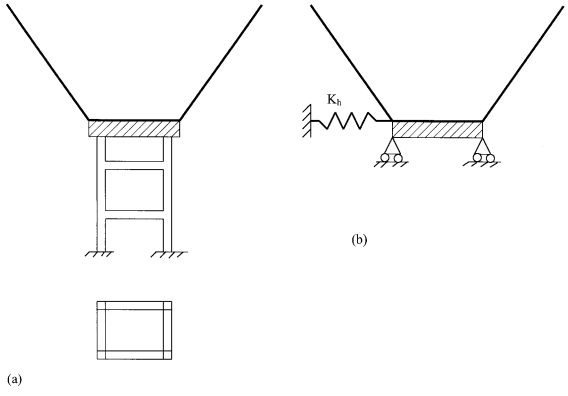

Figure 5. (a) Frame supporting a steel conical vessel; (b) spring simulating the supporting frame

the rigidity of the frames in the axial direction relative to the lateral direction. Consequently, the supporting tower can be replaced by a horizontal spring as shown in Figure 5(b).

The stiffness of the horizontal spring k_h is obtained by applying a horizontal force F_x at the top point of one of the rigid frames and using a plane frame program to calculate the corresponding lateral deflection Δ_x at that point. The stiffness k_h is then given by

$$k_h = \frac{2F_x}{\Delta_x} \tag{2}$$

In this analysis, both the walls and the base of the tanks are modelled using the consistent shell element. For the free axisymmetric vibration analysis, double symmetry exists and, therefore, 26 elements are used to model one-quarter of the tank. For the cases of non-linear time-history and lateral free vibration analyses, only symmetry about the axis of excitation exists. As such, one-half of each tank is modelled using 52 elements, 48 of which are needed to model the walls and four elements for the base. The finite element mesh employed is shown in Figure 6. It can be observed from the figure that a finer mesh is used at the bottom region of the tank where buckling is anticipated for the case of uniform thickness. The element lengths at the bottom region are chosen to be smaller than one quarter the buckling wavelength resulting from the static analysis.

Due to the rigid diaphragm action of the reinforced concrete slab, the displacement degrees of freedom of different nodes at the base of the tank are all assumed to be equal, when directed along the same axis. The

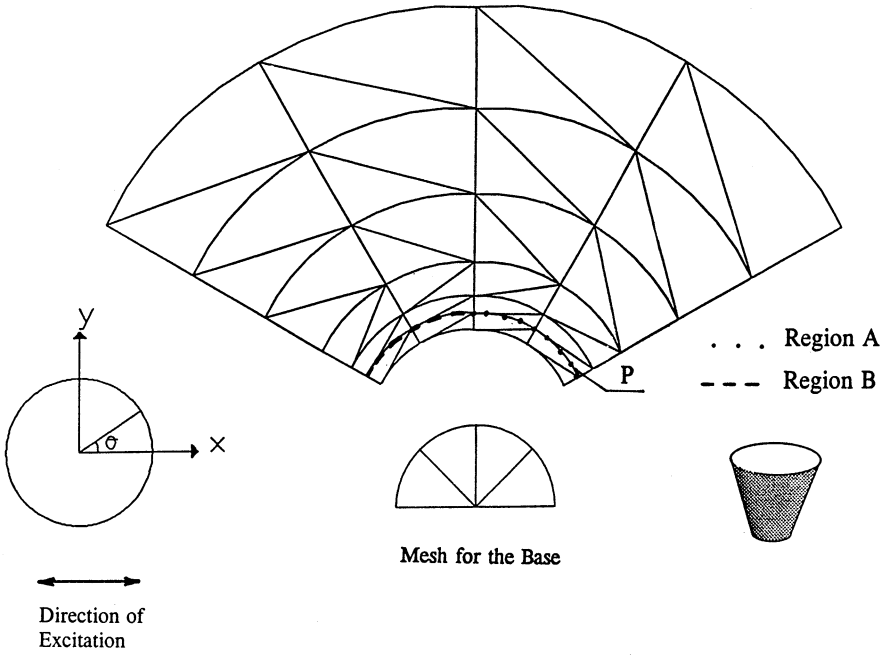

Figure 6. Finite element mesh for half cone

rotational degrees of freedom at the base are restricted because of the bending rigidity of the underlying reinforced concrete slab. A partial rotational restraint is expected to be provided by the weld connecting the base plate and the wall of the tank. However, in this study an assumption to neglect this effect was used and the wall of the tank was assumed to be free to rotate at its connection to the base.

7. STIFFNESS VALUE FOR THE SUPPORTING TOWERS OF THE TANKS

In order to perform seismic analysis for both the tall and the broad tanks, it is necessary to determine the stiffness of the spring k_h which simulates the supporting tower as described in Section 6. The preliminary analyses show that the fundamental frequencies of both the tall and the broad tanks are relatively high. This means that such structures will be more excited when subjected to an earthquake having a high peak acceleration to peak velocity ratio (a/v). According to the National Building Code of Canada NBCC,[13] Quebec city is located in an active seismic zone which can expect such an earthquake type of motion. Based on this, it is assumed that the tall and broad tanks are located there. Consequently, the reinforced concrete supporting frames of both tanks have to be designed to withstand the flexural stresses resulting from either the seismic load or the wind pressure intensity for that location, and in accord with the standard cited above. In addition, they must resist direct compressive stresses due to the weight of the liquid, the self-weight of the shell and its roof, and the snow load. The heights of the supporting towers for tall and broad tanks are assumed to be 10 and 6 m, respectively.

Some preliminary analyses show that for both the tall and broad tanks, the induced flexural stresses due to the seismic motion are much larger than those resulting from the wind pressure. The dimensions of the reinforced concrete frames for each tank are chosen based on the maximum compressive strength of concrete, assumed to be 13.3 MPa (based on 33.3 per cent of a 28-day nominal compressive strength of 40 MPa). Using the moment of inertia and the cross-sectional area values that confirm safe design for the supporting rigid

Table II. Natural frequencies f (cps) of tanks T1 and B1 due to horizontal and vertical excitations

Tank	Horizontal excitation				Vertical excitation			
	f_1	f_2	f_3	f_4	f_1	f_2	f_3	f_4
T1	2·51	3·54	6·67	12·04	7·44	14·95	19·06	24·46
B1	3·21	4·37	7·61	10·35	8·12	13·52	15·46	31·35

frames, the stiffness of the springs for modelling are calculated for each tank as given in equation (2). For Tall Tanks, k_h computes as $0{\cdot}708 \times 10^9$ N/m, while for Broad Tanks the value is $0{\cdot}220 \times 10^9$ N/m.

8. FREE VIBRATION ANALYSIS OF TALL AND BROAD TANKS

The tanks B1 and T1 were chosen for free vibration analysis. These two tanks, filled with water ($\rho_F = 1000\,\text{kg/m}^3$) were modelled using the consistent shell element, with the stiffness of the horizontal springs as noted above. Also required are the fluid added-masses $[DM]_H$ and $[DM]_V$ which are obtained for each tank following the procedures described in Sections 4.1 and 4.2 of the companion paper (El Damatty *et al.*[1]). Each added-mass is then individually incorporated into the free vibration analysis to obtain the natural frequencies of the tanks due to horizontal and vertical vibrations.

The results of the free vibration analyses show that considering only the first four modes of the pressure functions H_{i0} and H_{i1}, i.e. $i = 1$–4, gives sufficiently accurate values for the natural frequencies of the first four modes of vibration. This has been confirmed by considering only the first three pressure modes in the free vibration analysis, since the results remained almost the same as those obtained by including the fourth pressure mode. The natural frequencies from the free vibration analyses of both tanks using four pressure modes are shown in Table II.

9. TIME-HISTORY ANALYSIS FOR LIQUID-FILLED CONICAL TANKS

Tanks B1 and T1 to T6 were modelled using the consistent shell element for time-history analysis. The spring constants which simulate the supporting shaft of the broad tank (B1) and the tall tanks (T1–T6) are as given in Section 7. The fluid added-mass matrices $[DM]_H$ and $[DM]_V$ for both the broad and tall tanks, are calculated following the procedures outlined in the companion paper (El Damatty *et al.*[1]). Both $[DM]_H$ and $[DM]_V$ are added to the mass matrix of the shell to obtain the effective mass matrix $[M]$. To evaluate the damping matrix $[C]$ as a linear combination of the tangential stiffness matrix $[K_{Tan}]$ and the effective mass matrix $[M]$, the frequencies of the first two modes of vibrations must be known. For tanks B1, and T1–T3, the first two frequencies can be obtained from Table II. The free vibration analyses were performed for tanks T4, T5 and T6 resulting in the following values for the first two frequencies:

$$f_1 = 2{\cdot}63\,(\text{cps}), \quad f_2 = 3{\cdot}52\,(\text{cps}), \quad \text{(for tank T4)}$$

$$f_1 = 2{\cdot}68\,(\text{cps}), \quad f_2 = 3{\cdot}50\,(\text{cps}), \quad \text{(for tank T5)}$$

$$f_1 = 2{\cdot}83\,(\text{cps}), \quad f_2 = 3{\cdot}47\,(\text{cps}), \quad \text{(for tank T6)}$$

A time step Δt of 0·02 s was used in the analysis. The incremental solution at each time step Δt is obtained by solving the following equation:

$$[K^{*t(k-1)}]\{\Delta U\} = R^t - F^{t(k-1)} - [M]\{A^{t(k-1)}\} - [C]\{B^{t(k-1)}\} - [M]\{H\}a_H^t - [M]\{V\}a_V^t \qquad (3)$$

All variables of the above equation are defined in the companion paper (El Damatty *et al.*[1])

In order to obtain the non-linear time history of a liquid-filled tank subject to seismic motion, the following procedure is followed:

Constant quantities at start of solution. The following quantities are evaluated at the beginning of the solution and are kept constant throughout the subsequent time steps.

(a) The fluid added-masses $[DM]_H$ and $[DM]_V$ are evaluated using the procedure described in the companion paper and are added to the mass matrix of the tank $[M_S]$ to obtain the effective mass matrix $[M]$.
(b) The load vector $\{R^t\}$ due to the hydrostatic pressure acting on the walls of the tank, is calculated when it is filled with water, i.e. the load vector corresponding to a load factor $p =$ unity as described in Section 2.2.
(c) Assuming a 2 per cent damping and using the first two frequencies ω_1 and ω_2, obtained from the free vibration analysis of the liquid-filled tank, the coefficients α and β are evaluated by solving equations (55) and (56) given by El Damatty *et al.*[1]

Quantities updated at each time step. The components of the input ground acceleration a_H and a_V are updated at each time step according to the time history of the applied earthquake. The accelerations a_H^t and a_V^t are multiplied by the quantities $[M]\{H\}$ and $[M]\{V\}$, respectively, to obtain the load vectors resulting from the ground motion at time t.

Quantities updated at each iteration

(a) The stiffness matrices $K_L^{t(K-1)}$ and $K_S^{t(K-1)}$ and the unbalanced load vector $F^{T(K-1)}$ are updated at each iteration as described by El Damatty *et al.*[1,2]
(b) The vectors $\{A^{t(k-1)}\}$ and $\{B^{t(k-1)}\}$ are also updated at each iteration using equations (61) and (62), given in the companion paper.
(c) The stiffness matrices $K_L^{t(k-1)}$ and $K_S^{t(k-1)}$ are added together to obtain the tangential stiffness matrix $K_{Tan}^{t(k-1)}$ which is substituted in equation (54) (El Damatty *et al.*[1]), to obtain the damping matrix $[C]$.

The solution of equation (3) proceeds iteratively during each load increment corresponding to the time step Δt until equilibrium is achieved. A non-convergent solution at any iteration during the time history of the earthquake is an indication of dynamic instability due to the stiffness deterioration caused by yielding of the material and/or localized buckling. This means that the design of the tank being analysed is expected to be unsafe under the applied seismic excitation.

9.1. Choice of input ground motion

Non-linear time-history analysis of both the broad and tall conical-shaped reservoirs filled with water are performed using the San Fernando, California, February 1971 earthquake as the input ground motion.[14] In this study, the S74W component of the earthquake which was recorded at Pacoima Dam, is used as a horizontal excitation along the x-axis (see Figure 4), while the vertical component of the same record provides vertical accelerations. The reason for choosing this particular record as an input ground motion is that the dominant frequencies of such a record contain the fundamental modes of vibrations of the considered tanks. Only the strongest 6 s of the record are used in the analyses because of the very long computer time associated with this type of non-linear time-history analysis. The response spectra for the horizontal component of the ground acceleration for both the truncated and the full length records are plotted in Figure 7(a). A comparison between the acceleration response spectra for both the truncated and the full length records indicates excellent agreement up to a period of about 0·85 s. However, a long period

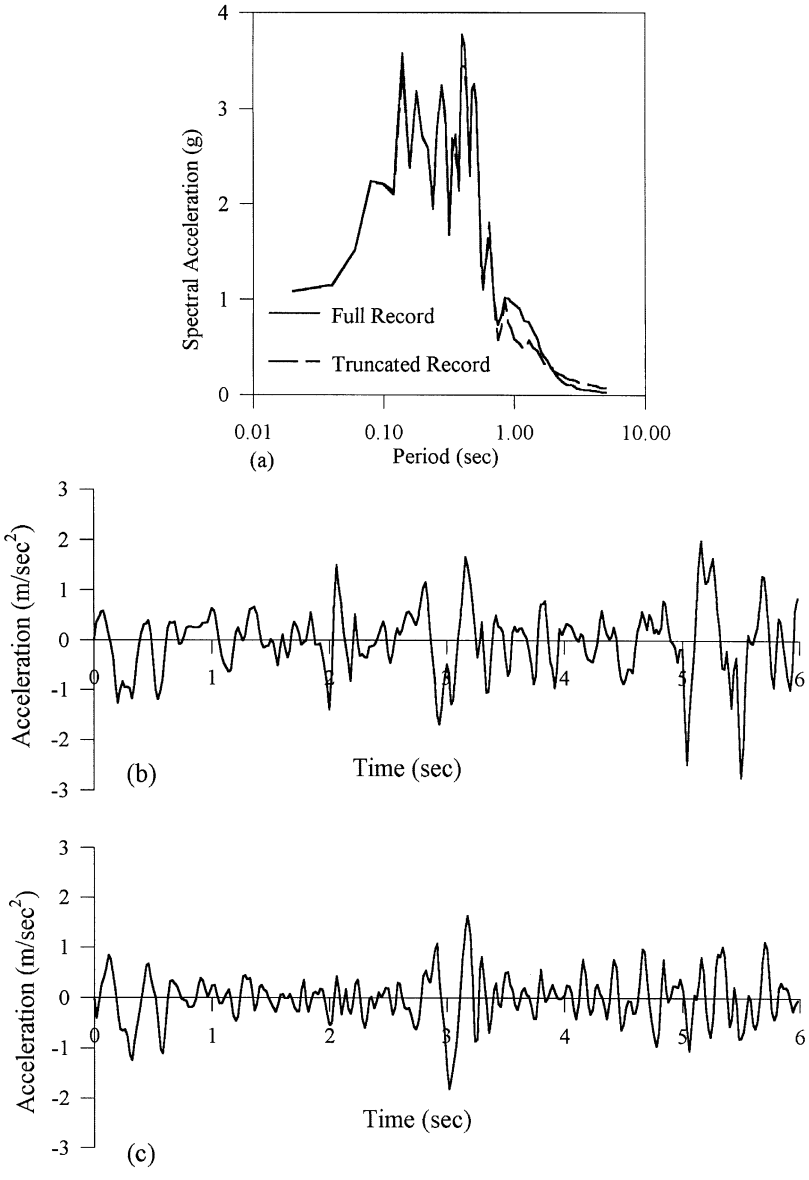

Figure 7. San Fernando earthquake Pacoima Dam S74W Record: (a) response spectrum 2 per cent damping; (b) scaled horizontal component of the ground acceleration; (c) scaled vertical component of the ground acceleration

acceleration varying between 0·85 and 2 s would be missed in the spectra of the truncated record. The time history of the full length record indicates that this long period excitation occurred at an early stage of the earthquake (which was not considered in the truncated record) with magnitudes too small to cause significant vibrations in the considered conical tanks (typical natural periods of these tanks are between 0·3 and 0·4 s, i.e. far from the excluded long-period excitation). Also there is no concern about plastification and the consequent increase in the natural period of the tank due to these small amplitude excitations. The

comparison between the response spectra of the full length and the truncated records also reveals that higher responses are obtained using the truncated record at periods exceeding 2 s. This can be anticipated due to the effect of the base line correction. This difference in the spectra can lead to an over estimated response of a tank after yielding. However, this will happen only when the yielded tank reaches a natural period of 2 s (i.e. having only about 40 per cent of its initial elastic stiffness). At this stage, such a tank would be expected to be severely damaged and to be on the verge of failure, in any event. As such we believe that truncating the record will have a minor effect on predicting the response of the considered tanks.

The two components of the acceleration records of the San Fernando earthquake are scaled down such that the maximum velocity of the input record is equal to the zonal velocity of Quebec City as specified in the NBCC.[13] This leads to maximum horizontal and vertical accelerations equal to $0{\cdot}280g$ and $0{\cdot}184g$, respectively, where g is the acceleration due to gravity. The scaled down horizontal and vertical components of the truncated record are shown in Figure 7(b) and 7(c).

9.2. *Discussion of results of the analysis*

Results of the time-history analysis are presented at three different generators of the tanks. These correspond to $\theta = 0^\circ$, $\theta = 90^\circ$ and $\theta = 180^\circ$ (see Figure 4). Note that the plane connecting the two generators $\theta = 0^\circ$ and $\theta = 180^\circ$, is parallel to the direction of horizontal excitation. It should also be pointed here that in the time-history plots, the response at $t = 0$ corresponds to the effect of the hydrostatic pressure before applying any seismic load to the structure.

The response of tank T1, which suffered from dynamic instability after exhibiting inelastic behaviour during the applied record, is presented in Figures 8 and 9. In Figure 8, horizontal, vertical, transverse meridional and axial displacements of the tank along the generator ($\theta = 0^\circ$) are displayed. In this figure, the dotted plots represent the displacement shapes resulting from the static load while the solid lines show the displacements just prior to dynamic instability. From the plots it can be observed that dynamic buckling, which is localized at the bottom of the tank, has the same pattern as that of the static displacements. Also to be noted, are the large horizontal and vertical movements at the upper region of the tank due to the seismic motion. In Figure 9, the same displacements are plotted along the generator ($\theta = 180^\circ$) of the tank. The displacement plots show no evidence of buckling along that generator. This means that buckling is localized near the base and is confined to the region subjected to high compressive axial stresses resulting from the overturning moment.

The response of the tall tank T5, which survived the earthquake without any inelastic behaviour is presented in Figures 10–13. The relative displacements along the x-axis at the top section of the tank are displayed in Figure 10, for $\theta = 0^\circ$, $\theta = 90^\circ$ and $\theta = 180^\circ$. It can be noted from these plots that the horizontal displacement take the cos θ-type variation, i.e. no out-of-roundness effect was noticed at any section of the tank. In Figure 11, the vertical displacements relative to the ground motion are also presented at the top section of the tank, for $\theta = 0^\circ$, $\theta = 90^\circ$ and $\theta = 180^\circ$. It is important to point out that the response at $\theta = 90^\circ$ is only due to the vertical acceleration, while the response at $\theta = 0^\circ$ and $\theta = 180^\circ$ results from both the vertical and the horizontal accelerations. It can be seen from the figures that the vertical displacements resulting from the horizontal excitation are larger than those resulting from vertical excitation, especially at the top section of the reservoir. The meridional stresses at the bottom section of the vessel are plotted in Figure 12 for $\theta = 0^\circ$, $\theta = 90^\circ$ and $\theta = 180^\circ$. Similar to the plots for vertical displacements, the results for stresses at $\theta = 90^\circ$ are only affected by the vertical acceleration, while the stresses at $\theta = 0^\circ$ and $\theta = 180^\circ$ are due to both the vertical and the horizontal components. From the plots of the stresses, it can be observed that the maximum stresses induced at the bottom section of the tank by the vertical acceleration are almost 32 per cent of the maximum stresses induced at the same section by the horizontal accelerations. It can also be observed that the stresses in the critical region due to the seismic motion are larger than those resulting from the hydrostatic pressure. In Figure 13, the time history of the base shear, normal force and overturning

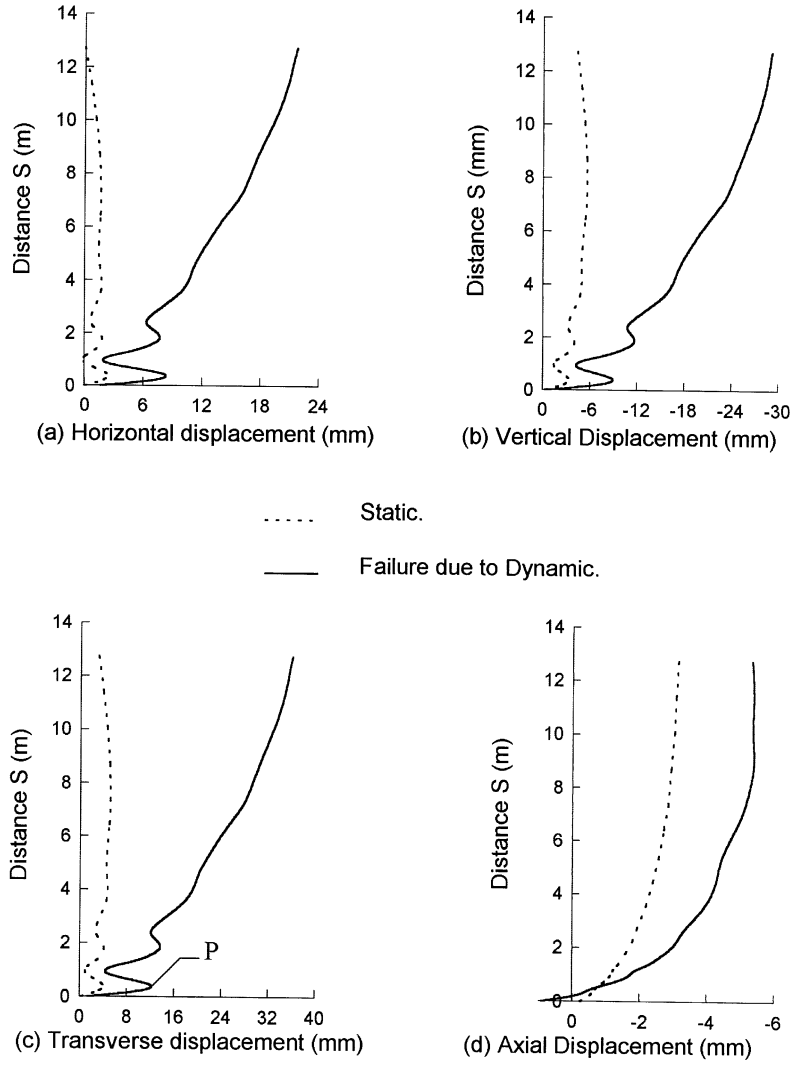

Figure 8. Displacement shape along the generator ($\theta = 0°$) of tank T1 at failure

moment at the bottom section of the tank are plotted. The normal forces are due to the effect of the vertical acceleration, while both the base shear and the overturning moment result from the effect of the horizontal acceleration. By simple calculation, the absolute base shear Q_{max}, normal force N_{max} are found to be related to the maximum ground horizontal acceleration ($a_H = 0{\cdot}28g$) and the maximum vertical acceleration ($a_V = 0{\cdot}184g$) through the mass of the fluid inside the tank M_F as follows: $Q_{max} = 0{\cdot}56\, M_F\, a_H$, and, $N_{max} = 2{\cdot}34 M_F\, a_V$.

The time history of the dynamic pressure resulting from the horizontal and vertical excitations was also calculated for different sections of tank T5 and is presented in the senior author's Ph.D. thesis.[15] Comparison of the numerical values indicates that the absolute value of the dynamic pressure resulting from the vertical acceleration is larger than the one resulting from the horizontal acceleration. Also, the analysis shows that

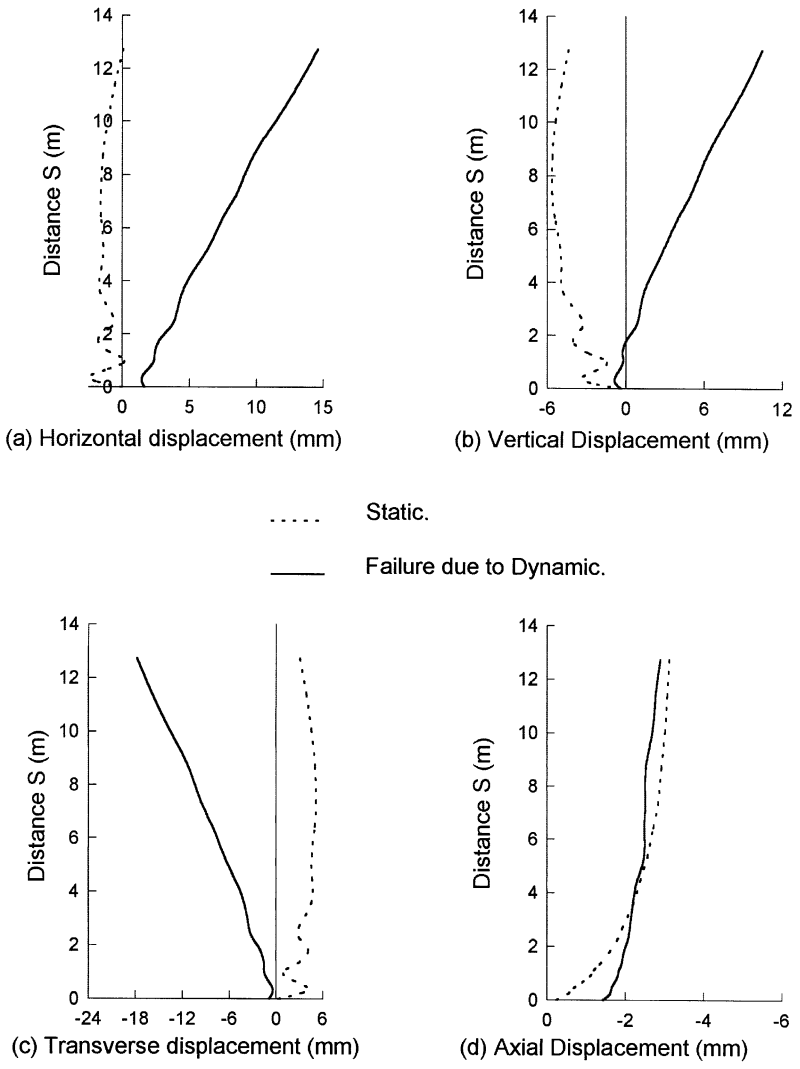

Figure 9. Displacement shape along the generator ($\theta = 180^\circ$) of tank T1 at failure

the absolute values of the dynamic pressure resulting from both excitations occur at different times as follows:

Maximum pressure due to horizontal excitation occurs at $t = 5{\cdot}46$ s.
Maximum pressure due to vertical excitation occurs at $t = 5{\cdot}1$ s.

Figure 14 shows the pressure distribution along the generator ($\theta = 180^\circ$) of tank T5. Figure 14(a) shows the distribution of the absolute dynamic pressure resulting from the horizontal acceleration (at $t = 5{\cdot}46$ s), while the absolute dynamic pressure due to vertical acceleration (at $t = 5{\cdot}1$ s) is displayed in Figure 14(b). In Figures 14(c) and 14(d), the absolute total dynamic pressure resulting from both the horizontal and the vertical excitations are plotted at $t = 5{\cdot}46$ s and $t = 5{\cdot}1$ s, respectively. It should be noted that in the last figures the dotted lines represent the hydrostatic pressure distribution. From these figures, it can be

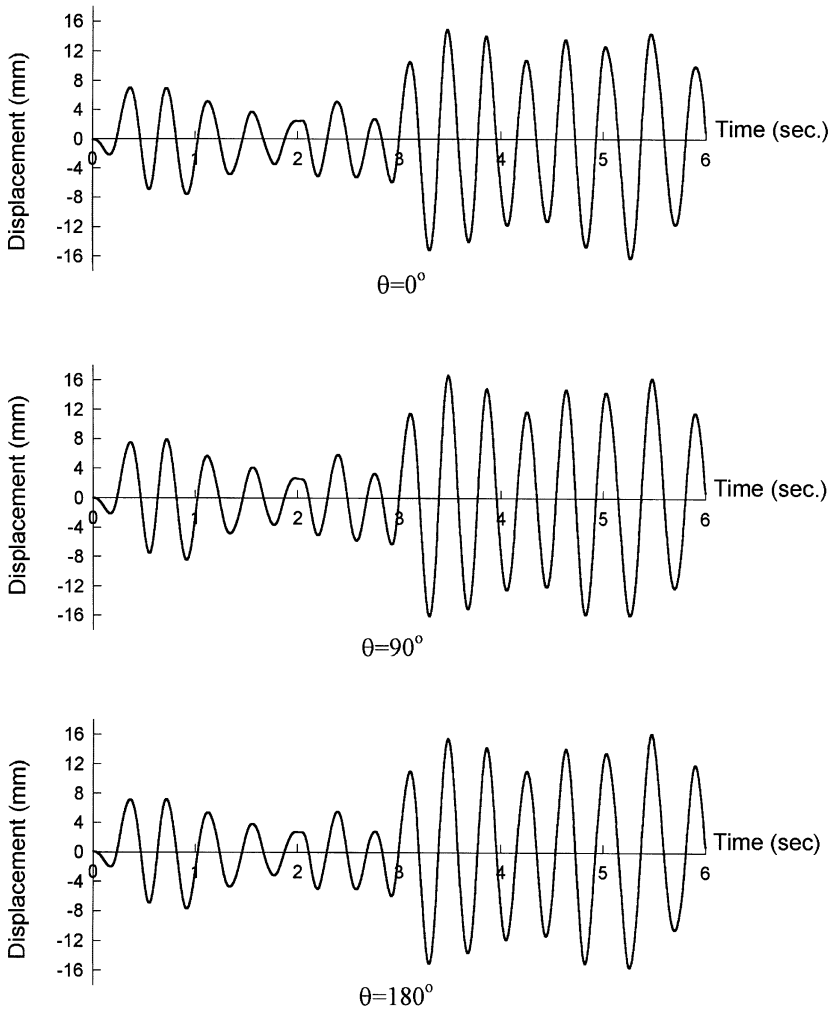

Figure 10. Time history of the relative displacements along the X-axis at the top section of tank T5.

concluded that the value of the total dynamic pressure is always less than the hydrostatic pressure. This means that no suction pressure is expected to happen at any point of the structure.

Both tanks T3 and T4 exhibited inelastic behaviour during the earthquake record. However, tank T4 survived the earthquake, while tank T4 failed during the 6 s record. To understand the difference in the behaviour of both tanks, a tracking of the spread of plasticity during the earthquake record is presented below for both tanks.

For tank T4, inelastic behaviour happened at $t = 5{\cdot}48$ s at the extreme fibres (i.e. a through thickness bending effect) of a localized part (region subjected to compression due to the overturning moment), located at the bottom of the cone. The structure had enough overall stiffness at that time to resist the loads and hence survived. During, the following load increments, the yielded fibres were subjected to unloading conditions, i.e. behaved elastically. No other part of the tank showed inelastic behaviour until the end of the earthquake record.

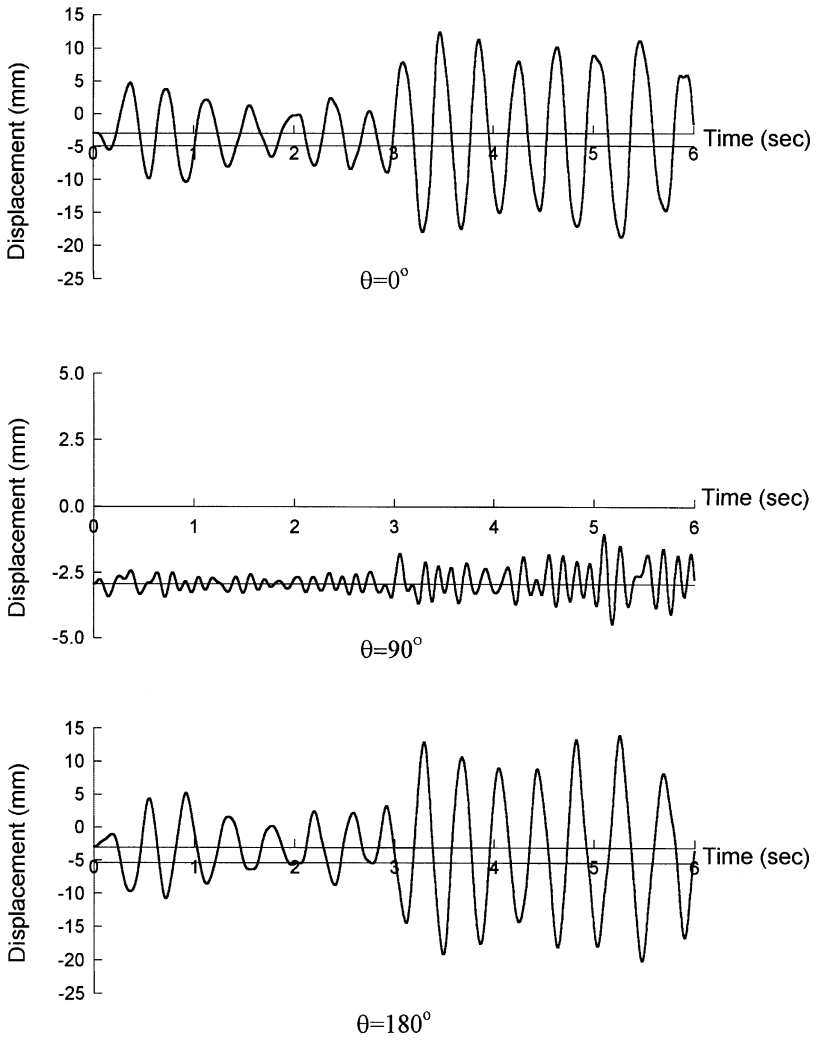

Figure 11. Time history of the relative vertical displacements at the top section of tank T5

The state of dynamic instability for tank T3, was associated with a buckling mode similar to the one exhibited by tank T1 and shown in Figure 8c. For such buckling mode, one would expect that most of the inelastic behaviour will be occurred at an annular segment located at the elevation of point P shown in Figure 8(c). One-half of this segment is shown in the finite segment mesh given in Figure 6 and is divided to two regions, A and B, which are denoted by the dotted points and the dashed lines, respectively. Under the action of the overturning moment resulting from the horizontal excitation, the mid-fibres of one region will be subjected to compressive meridional stresses while the mid-fibres of other region will be subjected to tensile meridional stresses. For the buckling shown in Figure 8(c), the inner and outer fibres for points located at the annular segment P will be subjected to compressive and tensile bending meridional stresses, respectively. Since the structure is initially subjected to through thickness uniform compressive meridional stresses due to static load, the largest meridional stresses will occur at the inner fibres of circle P. For tank T3, the inelastic behaviour took place after 5·34 s, when yielding occurred at the inner fibres of a localized part of region A. At $t = 5{\cdot}38$ s, yielding spread to cover region A entirely (still inner fibres only, i.e. through bending

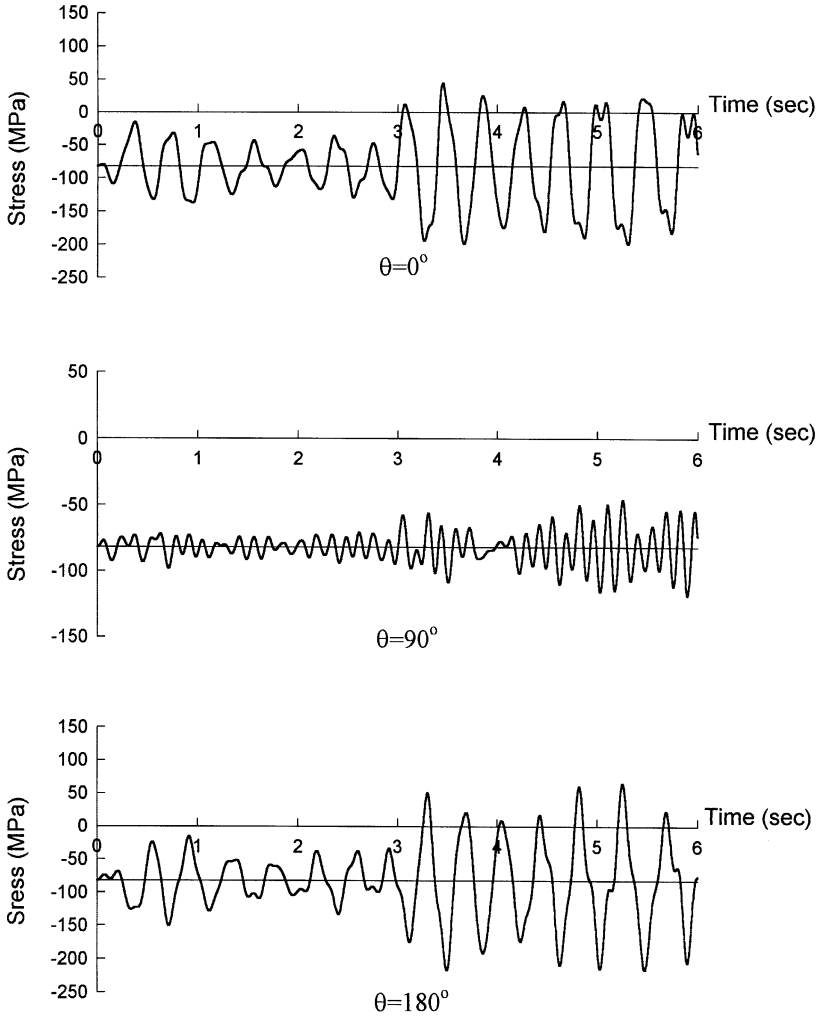

Figure 12. Time history of the meridional stresses at the bottom section of tank T5

effect). At $t = 5{\cdot}56$ the moment reversed, and yielding started at the inner fibres of the other side of the cone (region B). At $t = 5{\cdot}64$ s, region B showed unloading behaviour, while $t = 5{\cdot}82$ s, yielding again started at part region A. However, in this instance, plastic behaviour spread through the entire thickness. At $t = 5{\cdot}84$ s, the inelastic behaviour (through the entire thickness) spread to the whole circle P and together with the stiffness degradation due to the associated large deformations caused overall instability of the tank.

The broad tank B1 suffered from early plastification at the extreme fibers similar to the case of tank T4 while surviving the 6 s of the ground input acceleration. The results of the analysis of this tank are presented elsewhere in detail.[15] Similar response observations are found for B1 as noted above for tank T5. The former sustained noticeably smaller values for displacements and stresses due to the seismic motion. The absolute values for the base shear $Q_{\max}$ and the normal force $N_{\max}$ can be related to the mass of the fluid M_F as follows: $Q_{\max} = 0{\cdot}25 M_F a_H$ and $N_{\max} = 2{\cdot}20 M_F a_V$. Here a_H is the maximum input horizontal acceleration ($= 0{\cdot}28g$) and a_V is the maximum input vertical acceleration ($= 0{\cdot}184g$). It is obvious that the broad tank is subjected to

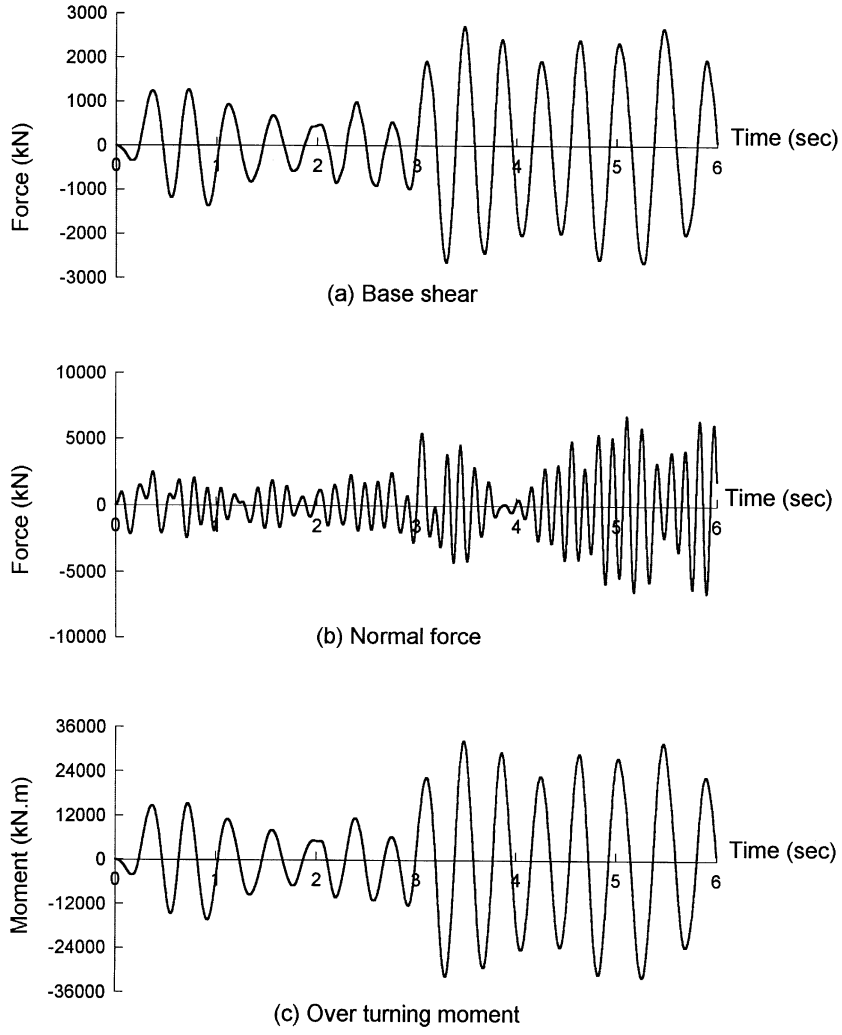

Figure 13. Time history of the base reactions at the bottom section of tank T5

somewhat less vertical force from the acceleration component a_V than does the tall tank. However, the base shear is very much reduced.

The results from the time-history analysis are summarized in Table I. The last column denotes the most critical state experienced by each structure during the 6 s of record. The term 'safe' denotes that the tank has survived the earthquake motion, while the tanks which have suffered from dynamic instability during the 6 s of the input ground motion are described by the term 'failed'. In the same column, tanks which have a complete elastic response during the record are described by 'elastic', while the term 'plastification' denotes the tanks which had an inelastic response during the seismic motion.

In light of the static limit load factor p_{cr} tabulated in the seventh column of Table I, the following observations can be concluded from the dynamic analysis:

(1) The broad tank investigated is much less critical to seismic load than are tall tanks. This is concluded from the fact that a limit load factor of 1·5 provides a safe design for the broad tank B1 under the input

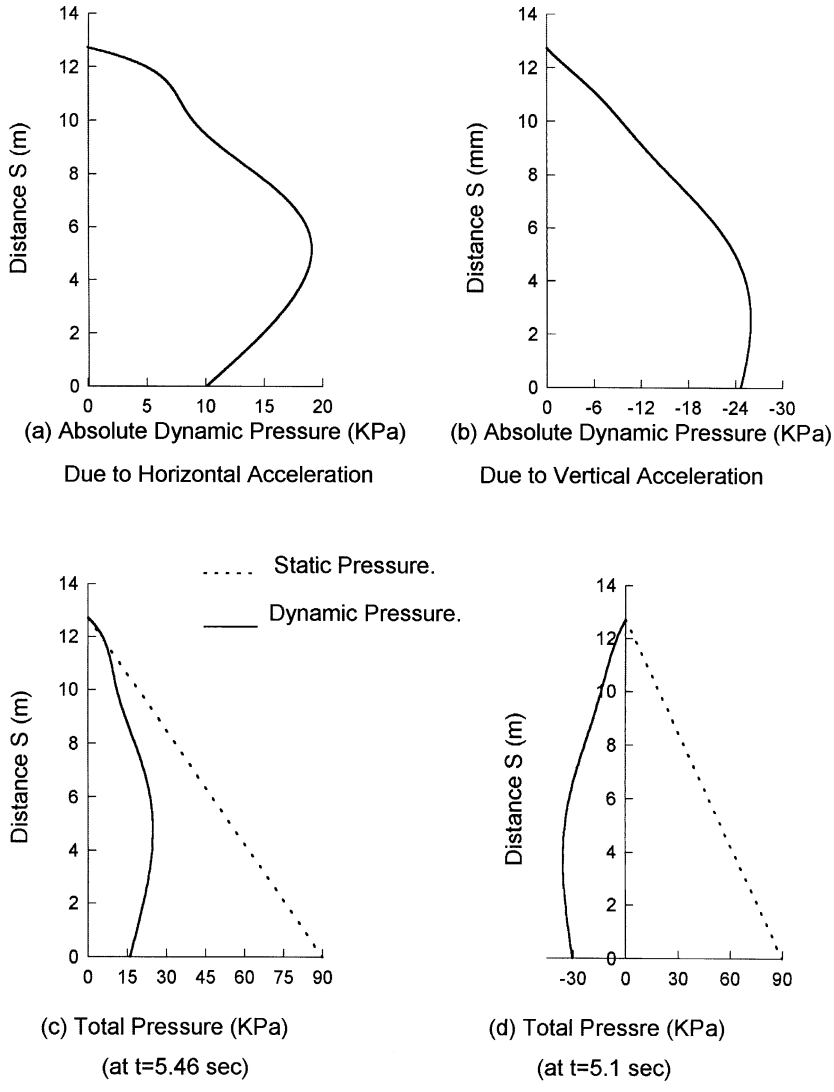

Figure 14. Pressure distribution along the generator of tank T5

ground motion, in spite of the early plastification which occurred in the extreme fibres of the lowest region of the cone. Meanwhile, the same seismic excitation applied to the tall tank T3 led to dynamic instability of the tank, despite a high load factor of 2·25.

(2) The results of the analyses of tanks T4, T5 and T6 show that under seismic excitation which has the frequency content of the fundamental modes of the tall tank and has a maximum acceleration equal to $0{\cdot}28g$, a load factor under static conditions of 2·8 has to be provided to assure the safety of the structure from dynamic instability, with a full elastic response. Meanwhile, a load factor of 2·65 leads to a safe inelastic response of the tall tank under the same excitation. These load factors can be achieved either by increasing the thickness of the tank or assuring a lower level of imperfections.

(3) A slight increase in the thickness of the tall tanks from 12 mm (tank T3) to 13·5 mm (tank T4) assured its safety under the applied seismic motion. Meanwhile, a reduction in the imperfection level from unit

thickness imperfection (tank T1) to an exactly perfect structure (tank T3) had no effect on the tall tank's overall seismic behaviour; both tanks suffered from inelastic behaviour followed by dynamic buckling. These observations give an indication that the increase of the thickness of a conical tank has a more significant effect than the reduction in the existing imperfection level when seismic analysis is considered. However, more parametric studies should be performed to generalize the above.

10. CONCLUSION

The seismic analysis presented in this paper represents the first attempt, to the best of authors' knowledge, to study the stability of liquid-filled conical tanks under earthquake loading. In this investigation, the consistent shell element has been used to model the steel vessel, while the boundary integral method was employed to obtain the impulsive component of the hydrodynamic pressure resulting from the horizontal and the vertical components of an earthquake.

The towers supporting liquid-filled conical tanks have been modelled using horizontal springs. The free vibration analyses of these elevated tanks indicate that the fundamental modes of vibration arise from the horizontal excitation. Thereafter, the non-linear time-history analyses of tall and broad conical tanks, using the horizontal and the vertical components for the San Fernando 1971 earthquake scaled down to meet the code specification for Quebec City, Canada, were carried out. These analyses reveal that, for a number of tall tanks, inelastic behaviour sets in during the earthquake record. This is followed by localized inelastic buckling near the base of the tank. This dynamic instability state occurs for tall tanks which are designed under a static load factor less than 2·65. Therefore, it can be concluded that the liquid-filled conical tanks, especially the tall superstructures, are very sensitive to seismic loading and must be designed for large static load factors in order to survive strong seismic motion. Meanwhile, the broad tank, designed for a static load factor of just 1·5, survived the earthquake in spite of early plastification. The compressive meridional stresses, which are the main cause of instability of conical tanks, are mainly caused by three effects: horizontal acceleration, hydrostatic pressure and vertical acceleration. The numerical results indicate that the largest contribution to these stresses comes from the overturning moment resulting from the horizontal acceleration. The second most important factor is the hydrostatic pressure. However, all three factors are important. The ratio of the maximum meridional stresses resulting from the vertical acceleration to the maximum stresses due to the horizontal acceleration is approximately one to three. Therefore, it is concluded that the vertical acceleration does contribute significantly to the dynamic instability of liquid-filled conical vessels and cannot be ignored in a seismic analysis of such structures. Analyses also show that a further gain the seismic strength of conical tanks can be achieved by increasing its thickness rather than by reducing the level of geometric imperfections. More parametric studies have to be conducted to prove the above observation conclusively.

APPENDIX

Notations

a_{H}^{t}	horizontal component of the ground acceleration at time t
a_{v}^{t}	vertical component of the ground acceleration at time t
$[C]$	damping matrix
$[DM]$	fluid added-mass matrix
$[DM]_{\mathrm{H}}$	fluid added-mass matrix resulting from the horizontal ground accelerations
$[DM]_{\mathrm{v}}$	fluid added-mass matrix resulting from the vertical ground accelerations
E, v	elastic modulus and poisson's ratio of the steel tanks
E_{T}	tangent modulus of the steel tanks

$\{F\}$	unbalanced load vector
h	height of the fluid in the conical vessel
K_h	stiffness of the horizontal spring simulating the supporting frames
K_v	stiffness of the vertical spring simulating the supporting frame
$[K_L]$	sum of the linear and the initial strain stiffness matrices
$[K_s]$	initial stress stiffness matrix
$[K_{Tan}]$	tangential stiffness matrix
$[M]$	effective mass matrix
$[M_s]$	mass matrix of the shell
p	static load factor
p_{cr}	critical static load factor
r_1	radius at the base of the cone
$\{R\}$	load vector due to hydrostatic pressure
S	distance measured along the generator of the cone
w_0	amplitude of the imperfection wave
θ_v	angle of inclination of the generator of the cone with the vertical
σ_y	yield stress of the steel tank

REFERENCES

1. A. A. El Damatty, F. A. Mirza and R. M. Korol, 'Stability of elevated liquid-filled conical tanks under seismic loading, Part I—Theory', *Earthquake Engng. Struct. Dyn.* **26**, 1191–1208 (1997).
2. AWWA, *AWWA Standard for Welded Street Tanks for Water Storage*, AWWA D100, Denver, Colorado, 1984.
3. J. L. Dawe, C. K. Seah and A. K. Abdel-Zaher, 'Investigation of the regent street water tower collapse', *AWWA J.* 315–323 (1993).
4. M. A. Haroun and H. M. Ellaithy, 'Seismically induced fluid forces on elevated tanks', *J. Tech. Topics Civil Engng.* **1**, 1–15 (1985).
5. M. A. Haroun and M. A. Tayel, 'Response of tanks to vertical seismic excitations', *Earthquake Engng. Struct. Dyn.* **13**, 329–345 (1985).
6. A. Niwa and R. W. Clough, 'Buckling of cylindrical liquid-storage tanks under earthquake loading', *Earthquake Engng. Struct. Dyn.* **10**, 107–122 (1982).
7. G. Manos and R. W. Clough, 'Tank damage during the May 1983 Coalinga Earthquake', *Earthquake Engng. Struct. Dyn.* **13**, 449–466 (1985).
8. G. Manos, H. Shibata and T. Shigeta, 'Correlation of cylindrical tank wall buckling with an earthquake motion recorded at a small distance from the tank', *Earthquake Engng. Struct. Dyn.* **18**, 169–184 (1989).
9. D. Vandepitte, J. Rathe, B. Verhegghe, R. Paridaens and C. Verschaeve, 'Experimental investigation of hydrostatically loaded conical shells and practical evaluation of the buckling load', in: *Buckling of Shells*, ed. E. Ramm, *Proc. State-of the-Art Colloquium*, Universitat Stuttgart, Germany, 1982, pp. 375–399.
10. A. A. El Damatty, F. A. Mirza and R. M. Korol, 'Stability of imperfect steel conical tanks under hydrostatic loading', *J. Struct. Engng. ASCE* **123**, 703–712 (1997).
11. B. Koziey and F. A. Mirza, 'Consistent thick shell element', *Comput. Struct.* (1996), March (1997).
12. A. A. El Damatty, R. M. Korol and F. A. Mirza, 'Large displacement extension of consistent shell element for static and dynamic analysis', *Comput. Struct.* **62**, 943–960 (1997).
13. National Building Code of Canada, *National Research Council of Canada*, *Ottawa*, 1990.
14. N. Naumoski, W. K. Tso and A, C. Heidebrecht, 'A selection of representative strong motion earthquake records having different A/V ratio', *Report EERG 88-01*, Earthquake Engineering Group, McMaster University, Hamilton, Ontario.
15. A. A. El Damatty, 'Non-linear dynamic extension of consistent shell element and analyses of liquid-filled conical tanks', *Ph.D. Thesis*, McMaster University, Hamilton, Ontario, Canada, 1995.

